Resonance-Enhanced Raman Identification of a Ternary Chemical Intermediate during the Equine Liver Alcohol Dehydrogenase Reduction of *p*-(Dimethylamino)benzaldehyde†

Paul W. Jagodzinski, Gerry F. Funk, and Warner L. Peticolas*

ABSTRACT: The nature of the binding of aromatic aldehyde and aromatic alcohol substrates to the catalytic zinc of equine liver alcohol dehydrogenase has been studied by using resonance-enhanced Raman spectroscopy. When an excess of both enzyme and coenzyme to substrate is used, a stable ternary chemical intermediate is formed between liver alcohol dehydrogenase and the reduced coenzyme, nicotinamide adenine dinucleotide, and the aldehyde, *p*-(dimethylamino)benzaldehyde, in the pH range 8.5–9.6. Resonance-enhanced Raman spectra clearly show that this same intermediate is formed between the excess enzyme, oxidized coenzyme, and the corresponding alcohol, *p*-(dimethylamino)benzyl alcohol. Thus, in the presence of excess enzyme and coenzyme, this specific ternary complex is a stable intermediate for both forward and reverse reactions. As a model for this enzyme–substrate intermediate, a complex between the aldehyde and Zn^{2+} in diethyl ether was made which showed a resonance-enhanced Raman spectrum essentially identical with that of the enzyme–coenzyme–substrate intermediate and completely different from that of the substrate. Most striking in this spectrum is the total absence of the carbonyl vibration which indicates that the C=O no longer exists in either the enzyme–substrate–coenzyme intermediate or the model complex, most probably due to the presence of a zinc–oxygen bond. The assignments are aided by ^{18}O isotopic substitution in the substrate. The Raman spectra of crystals of the ternary complex and the dynamics of the complex are also discussed.

The catalytic mechanism of liver alcohol dehydrogenase [EC 1.1.1.1 (LADH)[1]] has received considerable attention in the recent literature. Although the Theorell–Chance mechanism of ordered coenzyme and substrate binding and release is well accepted (Theorell & Chance, 1951), questions have been raised concerning the coordination number of the catalytic zinc and its role in substrate binding and hydride transfer (Fersht, 1977). Brändén and Theorell have made extensive use of inhibitors to mimic attachment of substrates to the protein (Theorell & McKinley McKee, 1961a,b; Boiwe & Brändén, 1977). Brändén and Eklund reported zinc–inhibitor bonds at the catalytic site and have inferred a direct binding of the substrate to the active-site zinc (Brändén & Eklund, 1978, 1980; Eklund et al., 1981; Plapp et al., 1978). Extensive studies of the pH dependence of LADH catalysis have led Kvassman & Pettersson (1978, 1980a,b) to concur with this model and support a direct coordination between substrate and catalytic zinc.

Dunn and his co-workers have employed the chromophoric substrate *p*-(dimethylamino)cinnamaldehyde (DACA) in their absorption spectral studies of chemical intermediates at elevated pH. They propose a coordinate bond between the active-site zinc and the substrate's carbonyl oxygen (Dunn & Hutchison, 1973; Dunn et al., 1975; Morris et al., 1980; Koerber et al., 1980). This conclusion is based on a red shift in the absorption spectra of the aldehyde *p*-(dimethylamino)cinnamaldehyde (DACA) when it is bound with the coenzyme to the enzyme. Although this suggestion is imaginative and stimulated the present investigation, it must be realized that red shifts in aromatic organic molecules, which are bound to proteins, may be due to a variety of reasons including the protein charge distribution at the site where the chromophore is bound which changes the nature of the electronic excited state. For example, the absorption spectra of rhodopsin and bacteriorhodopsin are enormously red shifted when compared to those of simple model compounds such as the Schiff bases of the corresponding retinal. However, the resonant Raman spectra of the proteins and the model compounds are essentially identical [for a recent review, see Honig (1978)].

Similarly, the absorption maxima of certain azo dyes such as methyl orange are shifted to the red by a large amount upon binding to human serum albumin (Klotz et al., 1952; Peticolas & Klotz, 1956). However, as Kim et al. (1975) have shown, in spite of the large red shift of the dye upon binding to the protein, its resonant Raman spectrum remains essentially unchanged. They correctly conclude that the red shift is due to a lowering of the excited electronic state of the dye and not any change in the ground electronic state. Thus, it is of interest to see what exactly is the origin of the observed red shift in the aromatic aldehydes upon binding to the LADH–NADH complex and to look at the model zinc–aldehyde complexes as has been done by Angelis et al. (1977).

An alternative model of substrate binding to LADH leaves the zinc-bound water molecule of the holoenzyme in place and binds the substrate to this water molecule via a hydrogen bond (Sloan et al., 1975; Drysdale & Hollis, 1980). These workers used the same substrate analogues (dimethyl sulfoxide and trifluoroethanol) employed in the X-ray studies to avoid the complication of unique results for a particular analogue.

Due to the difference in the conclusions obtained from X-ray and ultraviolet spectroscopic measurements on the one hand

† From the Department of Chemistry and the Institute of Molecular Biology, University of Oregon, Eugene, Oregon 97403. *Received October 23, 1981.* This work was supported by Grant PCM 76-82222 from the National Science Foundation and Grant GM-15547 from the National Institutes of Health.

[1] Abbreviations: DABA, *p*-(dimethylamino)benzaldehyde; DACA, *p*-(dimethylamino)cinnamaldehyde; DABOL, *p*-(dimethylamino)benzyl alcohol; LADH, equine liver alcohol dehydrogenase; NAD, nicotinamide adenine dinucleotide; NADH, reduced nicotinamide adenine dinucleotide; TCI, ternary chemical intermediate.

0006-2960/82/0421-2193$01.25/0

and NMR studies on the other, it seems important to obtain additional experimental evidence on this important problem in enzyme catalysis. Classical and resonance Raman spectroscopy are now common methods for studying proteins and enzyme–substrate interactions (Lord, 1977; Spiro & Gaber, 1977; Carey, 1978; McFarland et al., 1975). Although X-ray crystallographic measurements can determine such important factors as the distance between the zinc on the protein and the oxygen on the substrate, the actual nature of the electronic distribution or oxidation state of either the substrate or the coenzyme cannot be determined from X-ray diffraction.

We began our Raman studies of LADH in the hope of elucidating additional structural information about the ternary chemical intermediate (TCI). As we reported in our preliminary publication (Jagodzinski & Peticolas, 1981), stable intermediates involving aromatic aldehydes can generally be formed near pH 9.6. Similar complexes at high pHs have previously been reported by Dunn & Hutchison (1973). The substrate that we have used is the chromophoric aromatic molecule *p*-(dimethylamino)benzaldehyde (DABA) because it gives a very strong resonance-enhanced spectrum without fluorescence. Previous studies of LADH using DABA as a substrate have been carried out by Dworschack & Plapp (1977). The aldehyde DABA in the presence of the coenzyme NADH and catalytic amounts of the enzyme is readily converted into the corresponding alcohol. The LADH–NADH–DABA chemical intermediate can be modeled by the reaction of DABA with zinc chloride in nonaqueous solvents, similar to the transient chemical intermediate involving DACA (Angelis et al., 1977). This reaction can be represented

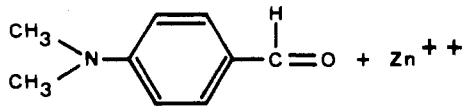

DABA

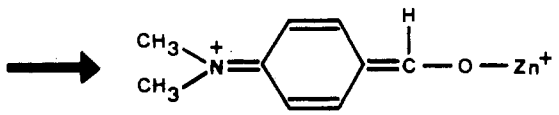

DABA–Zn Complex

Our earlier communication reported the Raman spectra of the ternary chemical intermediate (TCI) formed from LADH, NADH, and DABA in pH 9.60 pyrophosphate buffer and the DABA–Zn complex in methylene chloride (Jagodzinski & Peticolas, 1981). The close correspondence between the frequencies and intensities of the Raman lines for the two different species was noted, but no actual Raman spectra were shown.

In this paper, we report the detailed resonance-enhanced Raman studies of the TCI and a model complex in diethyl ether. However, we have extended the results considerably to show that the TCI is formed independently of whether one starts with the aromatic aldehyde and NADH or the corresponding aromatic alcohol and NAD^+. As we will show, in both cases, one obtains the same TCI with an excess of enzyme–coenzyme. Furthermore, at least some of the TCI is stable in the pH range from 8.5 to 9.6.

Experimental Procedures

Materials. Equine liver alcohol dehydrogenase (>98%) and reduced nicotinamide adenine dinucleotide (grade III, 98%) were purchased from Sigma Chemical Co. and used without further purification. *p*-(Dimethylamino)benzaldehyde was also purchased from Sigma and was stored in the dark over phosphorus pentoxide prior to use. Zinc chloride was purchased from Mallinckrodt, Inc., and was dried in vacuo and stored over phosphorus pentoxide until use or used immediately after drying.

p-(Dimethylamino)benzyl alcohol (DABOL) was prepared by the sodium borohydride reduction of DABA in a mixture of methanol and water. The resulting oil layer was isolated and distilled in vacuo, and a light yellow oil was obtained. NMR and UV–visible absorption spectra were used to check for any trace of the aldehyde. DABOL as a light yellow oil was stored below 0 °C to prevent decomposition: ^1H NMR ($CDCl_3$) δ 1.66 (s, 1 H), 2.92 (s, 6 H), 4.56 (s, 2 H), 6.68–7.26 (m, 4 H).

Anhydrous diethyl ether from J. T. Baker Chemical Co. was determined to be dry enough to be used without further purification. All nonaqueous solutions were prepared in an inert atmosphere. Aqueous buffer solutions were prepared from crystalline sodium pyrophosphate from Fisher Scientific Co.

Crystals of the TCI were grown from the usual solutions of the material: 1.4×10^{-3} N LADH, 10^{-3} M NADH, 7×10^{-4} M DABA. About 100 μL of this solution was stored open over 2-methyl-2,4-pentanediol at 4 °C in the dark until crystals appeared.

DABA with ^{18}O substitution at the carbonyl position was prepared by using the technique of first preparing the imine and then hydrolyzing to the carbonyl in $H_2{}^{18}O$ (G. F. Funk, P. W. Jagodzinski, and W. L. Peticolas, unpublished experiments).

Absorption and Raman Spectra. All absorption spectra were recorded by using a Cary Model 15 UV–visible spectrophotometer and quartz cuvettes. Raman and resonance Raman spectra were recorded as previously described (Gaber et al., 1978). The spectrometer was calibrated with indene (Loader, 1970), and the reported frequencies are expected to be accurate to ± 3 cm^{-1}. The 448.0-nm argon laser line was used for most of the spectra, but the 457.9-nm line was also used. Attempts to obtain true resonant Raman spectra by using the ultraviolet lines in the range 333–364 nm to date have only yielded fluorescence. The protein and TCI spectra were recorded with a 6-cm^{-1} slit width and the nonaqueous solvent model complex spectra with a 3-cm^{-1} slit width. The spectra of the protein-containing samples were recorded with the samples maintained at 4 °C to retard denaturation. Coadded spectra were smoothed as necessary by using standard methods (Savitski & Golay, 1964).

Results

The aromatic aldehyde DABA, like the similar substrate DACA, is reduced to its corresponding alcohol at increasingly slower rates as the pH is increased (Dunn & Hutchison, 1973; Jagodzinski & Peticolas, 1981), when the enzyme is present in catalytic amounts. In our initial work (Jagodzinski & Peticolas, 1981), we only studied the ternary complex at a pH of 9.6 and only complexes formed by the interaction of the coenzyme NADH and the aldehyde with a slight excess of the enzyme. However, more recently we have found that at enzyme–coenzyme:substrate ratios (10:1 → 2:1) far above the catalytic ratio (10^{-4}:1) the TCI is detectible in solutions anywhere in the pH range of 8.5–9.6. Furthermore, in molar excess of enzyme, the formation of the intermediate takes place with both the aldehyde and NADH as well as the alcohol and NAD^+. This indicates that on the surface of the protein when the coenzyme and substrate are both tightly bound, the low free energy component is the TCI. Under these conditions,

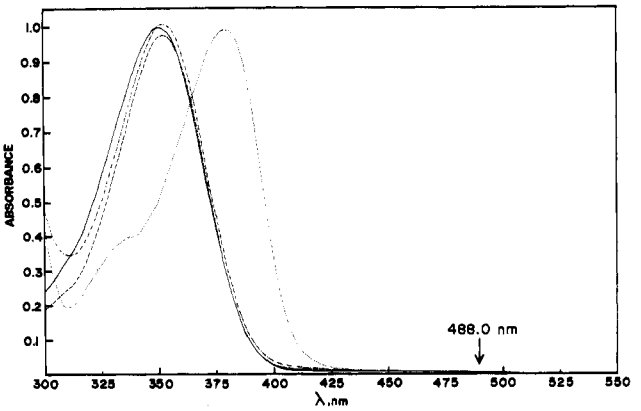

FIGURE 1: Comparison of the spectra of DABA (3.2×10^{-4} M) (---), DABA (2.7×10^{-4} M) and NADH (3.8×10^{-4} M) (—), and DABA (3.3×10^{-5} M) and LADH (6.4×10^{-4} M) (-·-·) with the spectrum of the intermediate (···) [DABA (3.3×10^{-5} M), NADH (4.3×10^{-4} M), and LADH (4.5×10^{-4} M) in pyrophosphate buffer (0.1 M), pH 9.6]. The spectra of DABA and DABA–NADH were taken with 0.1-cm path-length cells.

the intermediate appears to be more stable than either the products or the reactants. Most of our work was done by using the aldehyde and the NADH form of the coenzyme as starting materials, so consequently we begin with the description of these experiments.

The formation of the LADH–NADH–DABA ternary chemical intermediate was accomplished by adding an aliquot of a solution of DABA in appropriate buffer to solid NADH and an aliquot of the resulting solution to solid LADH. The order of addition of the components has been determined to have no effect on the kinetics of the reaction for aromatic aldehyde substrates (Dunn et al., 1979). The absorption spectra of DABA (λ_{max} 352 nm, $\epsilon = 3.0 \times 10^4$ M^{-1} cm^{-1}) and the TCI (λ_{max} 380 nm, $\epsilon \geq 2.9 \times 10^4$ M^{-1} cm^{-1}) are presented in Figure 1. The spectrum of the intermediate was recorded against an LADH–NADH blank of the same concentration so as to remove the contributions due to enzyme and coenzyme. The red-shifted absorption maximum of the TCI is attributed to an electron density rearrangement to the quinoid-like structure shown in the above schematic reaction. DABA was mixed with LADH and NADH separately to test the origin of this new absorption band. The absorption band of DABA did not shift to the red, and its shape was affected to only a minor extent in both cases. The spectra of NADH–DABA and LADH–DABA are also shown in Figure 1. Since the absorption maximum of the alcohol will be blue shifted, we therefore conclude that the new band at 380 nm must be due to an intermediate different in electronic structure from either DABA or DABOL.

The Raman spectra of DABA, the LADH–NADH–DABA ternary chemical intermediate, and the LADH–NADH binary complex taken with the 488-nm argon line are shown in Figure 2. As can be seen from the degree of resonance enhancement, DABA has undergone a considerable change in the nature of its chemical structure and bonding. Although the absorption band has no significant intensity beyond 430 nm, the enhancement of the spectrum of the TCI indicates that preresonance Raman effects occur at 488 nm, the wavelength of the exciting laser line. The spectrum of the LADH–NADH binary complex shows that Raman lines near 1670, 1450, 1300, and 1000 cm^{-1} may be assigned to the nicotinamide portion of the NADH (Rodgers & Peticolas, 1980; Bowman & Spiro, 1980), and the lines near 1000 cm^{-1} are assigned to the phenylalanine and tryptophan residues of the protein (Lord & Yu, 1970; Simons et al., 1972). Experiments have shown that the

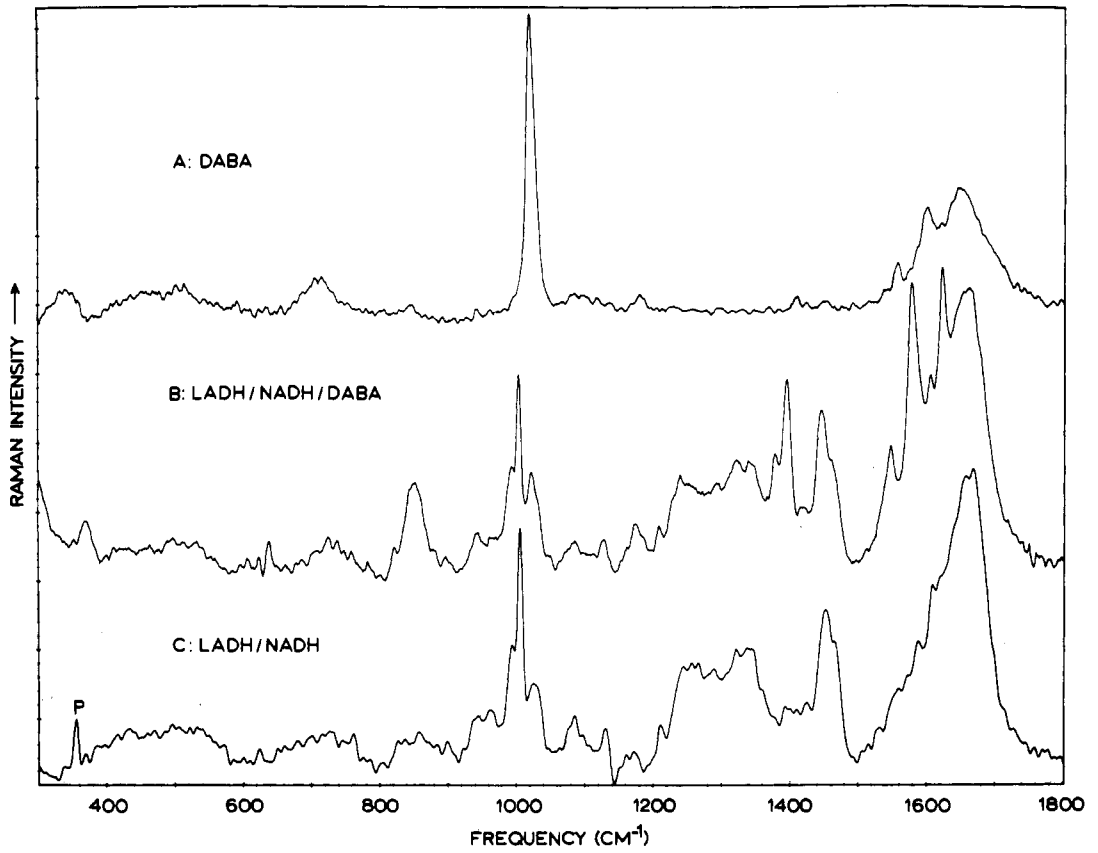

FIGURE 2: Raman spectra of 6.7×10^{-4} M DABA (trace A), 6.7×10^{-4} M DABA, 1×10^{-3} M NADH, and 1×10^{-3} M LADH (trace B), and 1×10^{-3} M NADH and 1×10^{-3} M LADH (trace C). The strong line near 1020 cm^{-1} in all spectra is due primarily to 0.1 M, pH 9.16, pyrophosphate buffer (P, plasma line).

Table I: Observed Raman Lines (cm^{-1}) for DABA and DABA-Zn in Diethyl Ether and for LADH-NADH-DABA and LADH-NADH in Aqueous Pyrophosphate Buffer

diethyl ether		pyrophosphate buffer[a]			
DABA	DABA-Zn	LADH-NADH-DABA	LADH-NADH	DABA	assignments
1696 (7)[b]					
		1663 (10)[c]	1667 (10)		C=O str
				1640 (4)	H_2O bend
	1624 (10)	1623 (4)			C=C str, C=N str
1605 (10)		1606 (1)		1595 (2)	ring
	1580 (5)	1579 (6)			ring
1564 (3)				1551 (1)	ring
	1546 (2)	1547 (2)			C=N str,[d] C=C str
1531 (1)					
		1467 (3, sh)	1465 (4)		
		1445 (6)	1451 (5)		
1439 (2)	1451 (3)				
		1425			
1419 (1)					
1394 (1)	1401 (10)	1396 (6)	1407 (1)		C=N str
1371 (1)	1377 (4)	1330 (2)			
	1359 (4)				
		1340 (1)	1337 (3)		
	1330 (1)	1325 (2)			
	1275 (1)				
			1260 (3)		
1243 (2)					
	1230 (1)	1240 (2)			
		1210 (1)	1210 (1)		
1170 (7)	1180 (2)			1179 (1)	
		1174 (1)	1175 (1)		
		1127 (1)	1130 (2)		
1127 (1, sh)					
	1092 (2)				
		1085 (1)	1085 (2)		
		1021 (4)	1025 (2)	1023 (10)	pyrophosphate buffer
		1004 (8)	1005 (8)		LADH (Phe, Trp)
	997 (2)				C-O str, CH wag
		995 (4)	997 (4)		
		962 (7)	962 (2)		
974 (1)	942 (1)	944 (2)			
	904 (1)				
	872 (1, sh)				
			856 (1)		
	847 (2, sh)	852 (4)			
838 (2)					
	787 (1)				
732 (3)	735 (1)				
		724 (2)	726 (7)		
639 (1)	643 (2)	638 (1)			
598 (1)	617				
	501 (1)				
			495 (1)		
444 (1)	444				diethyl ether
	394 (3)	368 (1)			Zn-O str tentative
					plasma line
355 (1)			355 (2)		
	319 (3)				

[a] Pyrophosphate buffer (0.1 M), pH 9.6. [b] Relative intensities in parentheses; sh = shoulder. [c] This intensity is anomalously high due to contributions from LADH and NADH (E. G. Rodgers and W. L. Peticolas, unpublished results). [d] Possibly due to delocalization in the ground state of DABA. All assignments taken from comparison with Raman spectra of similar quinoid structures; see Forster et al. (1980) and Machida et al. (1974).

pyrophosphate buffer contributes to the line at $\simeq 1020$ cm^{-1}. The spectra of the DABA–Zn complex in ether and in water indicate that the high-frequency shoulder at $\simeq 1460$ cm^{-1} is possibly due in part to the TCI. The observed frequencies for DABA, the LADH–NADH binary complex, and the LADH–NADH–DABA ternary chemical intermediate are presented in Table I. The assignments will be discussed below.

It has been proposed that Lewis acid complexes are reasonable models for ternary chemical intermediates involving LADH (Angelis et al., 1977). Our previous report of a DABA–Zn complex in methylene chloride has shown that indeed this is a very realistic model (Jagodzinski & Peticolas, 1981). However, we have found that at low DABA concentrations ($\simeq 10^{-3}$ M) this aldehyde does not compete effectively with methylene chloride to form inner-sphere complexes with zinc so that UV absorption spectra were difficult to obtain in this solvent. To circumvent this problem, we have used diethyl ether as the solvent in order to achieve as nearly as possible the stoichiometric formation of the metal–aldehyde complex. This is difficult because we have also found that there is a critical concentration beyond which the complex will precipitate in either diethyl ether or methylene chloride. The ab-

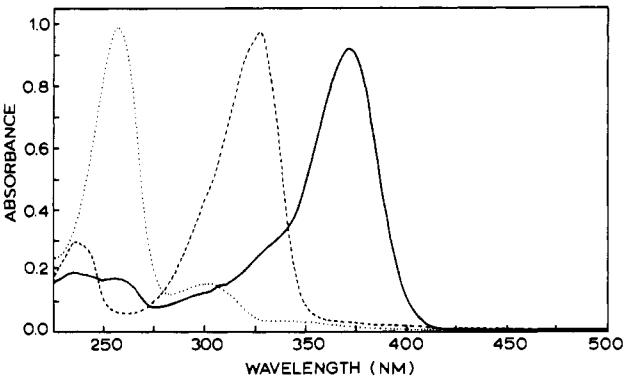

FIGURE 3: Comparison of the absorption spectrum of DABA (5.8×10^{-4} M) (---) with the spectrum of the Lewis acid complex (—) formed on addition of excess zinc chloride to DABA (4.0×10^{-4} M) and the spectrum of DABOL (1.1×10^{-3} M) (···). All samples were in diethyl ether, and the spectra were collected with 0.05-cm pathlength cells.

sorption spectra of DABA (λ_{max} 327 nm, $\epsilon = 3.2 \times 10^4$ M^{-1} cm^{-1}), the DABA–Zn complex (λ_{max} 372 nm, $\epsilon = 4.5 \times 10^4$ M^{-1} cm^{-1}), and DABOL (λ_{max} 257 nm, $\epsilon = 1.7 \times 10^4$ M^{-1} cm^{-1}) in ether are presented in Figure 3. The shift in absorption maxima from 327 to 372 nm is consistent with the formation of a quinoid-like structure upon binding to Zn^{2+}. It should be noted that the absorption maxima of the TCI and DABA–Zn complex are very similar, but the TCI absorption spectrum is also due to a contribution from bound NADH which falls in this region.

The Raman spectra of DABA and its Lewis acid complex in diethyl ether are displayed in Figure 4. The similarity of the Raman spectra of the TCI and the Lewis acid complex is apparent (Table I). There are a number of strong Raman frequencies which dominate the spectra of the Zn–DABA complex and the TCI but which are absent in either the DABA or the DABA–LADH spectra. Among these are the strong peaks at 1625, 1580, 1546, and 1401 cm^{-1} in ether and 1623, 1579, 1547, and 1396 cm^{-1} in the TCI. These are the marker bands for the zinc-induced quinoid form of the substrate. They are observed for the Zn–DABA complex in organic solvents and in the TCI at pH 9.6. If sufficient water is added to the organic solvents, the spectrum of uncomplexed DABA is recovered. The Raman spectrum of DABOL in ether is shown in Figure 5. Comparison of trace B in Figure 4 with Figure 5 again indicates that we have not formed the product alcohol, DABOL, which in any event would not be expected to give a resonance-enhanced Raman spectrum as its absorption is in the ultraviolet.

Perhaps the most significant change in the DABA spectrum upon complexation with the zinc is the disappearance of the

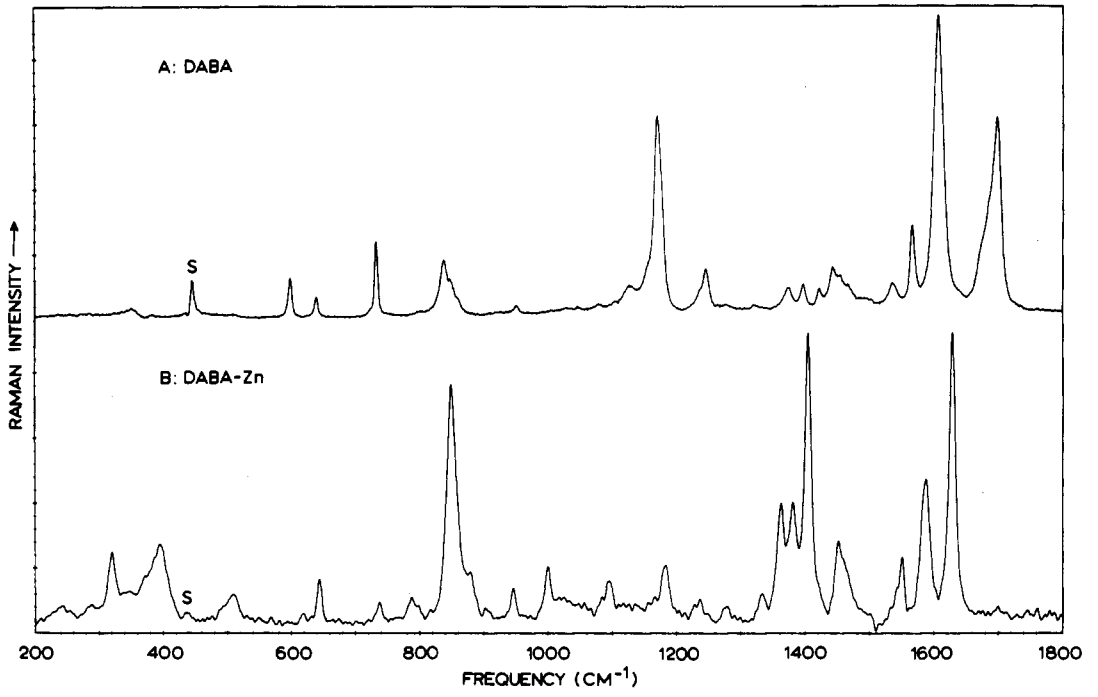

FIGURE 4: Raman spectra of $\simeq 3 \times 10^{-2}$ M DABA (trace A) and $\simeq 3 \times 10^{-2}$ M DABA–Zn complex (trace B) in diethyl ether (S, computer-subtracted solvent line).

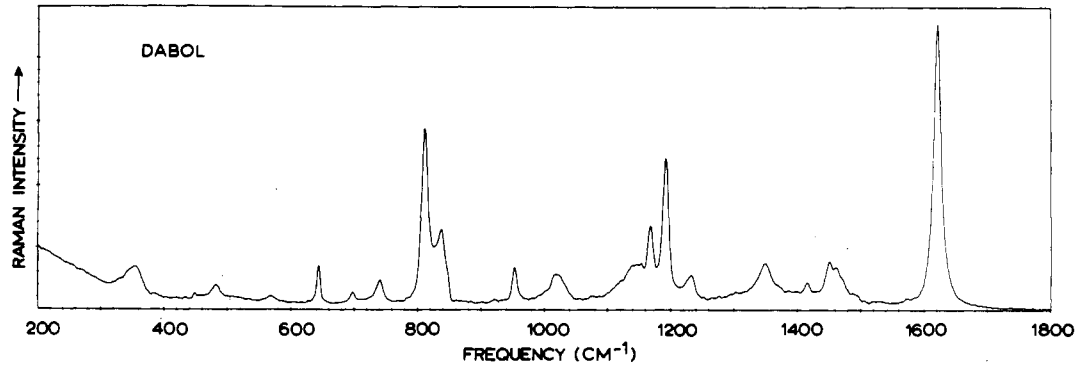

FIGURE 5: Raman spectrum of DABOL (7×10^{-1} M) in diethyl ether with the solvent lines computer subtracted.

Table II: Observed Raman Frequencies for (^{18}O)DABA and Its Complex with Zn^{II} in Methylene Chloride

(^{18}O)DABA (cm^{-1})[a]	$\Delta\nu$[b] (Δcm^{-1})	(^{18}O)DABA-Zn (cm^{-1})[a]	$\Delta\nu$[b] (Δcm^{-1})	assignments
1646 (5)[c]	21	1646 (1)[c]	0	C=O str
		1621 (7)	8	ring, C=C str, C=N str
1600 (10)	2			ring
		1587 (10)	5	ring
1556 (3)	3			ring
		1547 (5)		C=N str,[d] C=C str
1533 (1)	2			
1440 (1)	2	1445 (4)	0	
1418 (1)	1	1419 (1)	0	
1389 (2)	9	1393 (9)	9	C-N str tentative
1376 (1)	0	1374 (10)	5	
		1355 (3)	−1	
		1327 (1)	1	
1245 (1)	1			
		1234 (1)	0	
1170 (5)	1	1173 (4)	0	
		999 (1)	1	C-O str tentative
949 (1)	−1	945 (1)	1	
		846 (10)	0	
836 (1)	1			
730 (2)	2	733 (3)	3	
706 (3)	0	706 (6)	0	CH_2Cl_2 solvent
637 (1)	1	638 (5)	3	
593 (1)	6	607 (2)	7	C=O wag
		500 (1)	0	
		382 (5)	1	
353 (1)	−1			
		309 (2)	−2	

[a] Peaks relative to 706-cm^{-1} methylene chloride band. [b] $\Delta\nu = \nu[(^{16}O)DABA] - \nu[(^{18}O)DABA]$. [c] Relative intensities in parentheses. [d] Possibly due to delocalization in the ground state of DABA.

Table III: Observed Raman Frequencies for (^{18}O)DABA and Its Complexes with Zn^{II} in Diethyl Ether

(^{18}O)DABA (cm^{-1})[a]	$\Delta\nu$[b] (Δcm^{-1})	(^{18}O)DABA-Zn (cm^{-1})[a]	$\Delta\nu$[b] (Δcm^{-1})[c]	assignments
1656 (5)[d]	40			C=O str
		1625 (10)	−1	C=O str, C=N str
1605 (10)	0			ring
		1582 (7)	2	ring
1563 (4)	0			ring
		1547 (3)	−1	C=N str,[e] C=C str
1533 (1)	2			
1439 (2)	1	1448 (5)	3	
1420 (2)	−1			
1387 (2)	7	1401 (10)	0	C-N str
1372 (2)	−1	1378 (6)	−1	
		1359 (5)	0	
		1329 (2)	1	
		1276 (1)	−1	
1243 (2)	0			
		1233 (1)	−3	
1171 (5)	−1	1180 (2)	0	
1126 (1)				
		1092 (1)	0	
		998 (2)	−1	C-O str
950 (1)	−3	944 (1)	−2	
		905 (1)	−1	
		847 (8)	0	
839 (2)	1			
		784 (1)	3	
731 (2)	1	735 (1)	0	
638 (1)	1	643 (2)	0	
593 (1)	5	619 (1)	−2	C=O wag
		508 (1)	−1	
444 (1)	0	444 (1)	0	diethyl ether solvent
		394 (3)	0	
		318 (1)	1	

[a] Peaks relative to 444-cm^{-1} diethyl ether band. [b] $\Delta\nu = \nu[(^{16}O)DABA] - \nu[(^{18}O)DABA]$. [c] The absence of any significant shifts indicates the ^{18}O has been exchanged in the Zn^{II} complex with ^{16}O from trace amounts of water in the ether. However, $^{18}O \rightarrow {}^{16}O$ exchange never occurs in the absence of Zn^{II}. [d] Relative intensities in parentheses. [e] Possibly due to delocalization in the ground state of DABA.

carbonyl band. This band appears at 1664 cm^{-1} in methylene chloride (Jagodzinski & Peticolas, 1981) but shows a remarkable shift to 1698 cm^{-1} in ether. In both solvents, this band disappears upon complexation with zinc, and a completely new band appears at 1626 cm^{-1}. The latter band does not change significantly upon $^{16}O \rightarrow {}^{18}O$ substitution, and consequently it cannot be assigned to a simple carbonyl vibration (see Discussion and Tables II–IV).

The appearance of many new Raman bands in a ligand upon metal complexation is novel since infrared and Raman studies of a large number of metal–ligand complexes show that the general rule is that the vibrational frequencies of ligands bound to metals change only a few wavenumbers, if at all, upon intershell coordination [see, for example, Nakamoto (1978)]. The complete absence of the carbonyl vibration in the zinc–DABA complex is thus striking and can only be interpreted with the reasonable assumption of the strong zinc–oxygen bond formation. The quinoid marker bands which appear in the DABA–Zn complex also appear in the TCI. These are listed in Table I. Of particular interest are the very strong bands at 1626 and 1548 cm^{-1} which show that the zinc–DABA complex in both ether and methylene chloride gives new bands identical with that observed in the enzyme complex. Thus, we may infer that there is no carbonyl band in the TCI where DABA is complexed to the catalytic zinc of LADH in the presence of NADH. This inference is indirect because it is made from comparison with the zinc–DABA complex. Because of the existence of amide carbonyl groups in both the protein and the coenzyme, Raman bands in the 1640–1670-cm^{-1} region are present in the enzyme and coenzyme. The Raman band of the coenzyme at 1660 cm^{-1} is resonance enhanced due to the coenzyme absorption band which overlaps that of the TCI (Rodgers & Peticolas, 1980; Bowman & Spiro, 1980). Thus, it is apparent that with NADH present one will always observe a carbonyl band in the Raman spectrum of the LADH–NADH–DABA mixture. The absence of the DABA carbonyl group in the enzyme–substrate complex may be inferred from the presence in the TCI of the strong quinoid form marker bands which are also found in the zinc–DABA complex in organic solvents where the carbonyl band is absent.

The Zn–DABA complex shows a new band at 398 cm^{-1} while the TCI shows a new band in the region of 369 cm^{-1}. Neither of these bands is present in the DABA spectrum in organic solvents nor in the LADH–NADH mixtures in aqueous solution without DABA. In our previous work (Jagodzinski & Peticolas, 1981), we tentatively assigned these vibrations to zinc–oxygen bond stretching because 390 cm^{-1} is a characteristic Zn–O stretching frequency. However, the possibility of a low-frequency ring mode was also discussed. In order to determine the nature of this low-frequency band, we have prepared and studied (^{18}O)DABA. This isotopic substitution at the carbonyl oxygen causes the frequency of

Table IV: Observed Raman Frequencies for (^{18}O)DABA in the LADH-NADH-DABA Ternary Complex in $H_2{}^{16}O$ and $H_2{}^{18}O$ Pyrophosphate Buffer[a]

LADH-NADH-(^{18}O)DABA (cm^{-1})	$\Delta\nu$[b] (Δcm^{-1})	assignments
1665 (8)[c]	−2	C=O str
1622 (1)	1	C=O str, C=N str
1592[d] (6)	3	ring
1576 (6)	3	ring
1548 (6)	−1	C=N str,[e] C=C str
1461 (1, sh)	6	
1445 (5)	0	
1390 (6)	6	C-N str
1371[f] (5)	9	
1326 (1)	−1	
1234 (1)	6	
1208 (1)	2	
1177 (4)	−3	
1129 (1)	−2	
1087 (3)	−2	
1023 (10)	−2	pyrophosphate buffer
1005 (5)	−1	LADH (Phe, Trp)
965 (1)	−3	
946 (2)	−2	
851 (6)	−1	
729[g] (3)	−5	
636 (1)	2	
368 (1)	0	

[a] Pyrophosphate (0.1 M), pH 9.0–9.3, in $H_2{}^{18}O$ solvent; frequencies of the LADH-NADH-(^{18}O)DABA intermediate in $H_2{}^{16}O$ gave no changes larger than 2 cm^{-1}, indicating $^{18}O \rightarrow {}^{16}O$ reexchange had occurred. [b] $\Delta\nu = \nu[(^{16}O)DABA] - \nu[(^{18}O)DABA]$ in LADH-NADH-DABA intermediate. [c] Relative intensities in parentheses. [d] This band is attributed to free DABA in aqueous solution. [e] Possibly due to delocalization of the ground state of DABA. [f] This band may be the ^{18}O-shifted cm^{-1} band, or it may have a contribution from uncomplexed DABA in the hydrophobic pocket of the protein (see Table III and Table II for DABA frequencies in this range in diethyl ether and methylene chloride). [g] Possibly a combination of uncomplexed (^{18}O)DABA (733 cm^{-1}) (in aqueous solution or the hydrophobic region of the protein) and the 724-cm^{-1} band of LADH-NADH-DABA.

a vibration which involves large displacements of the oxygen atom to show a pronounced shift to a lower frequency while other vibrations such as ring vibrations should show only small shifts. Thus, this study permits us to verify the assignment of the 1664-cm^{-1} DABA band in methylene chloride and the 1690-cm^{-1} band in ether as solvent-dependent carbonyl vibration frequencies as well as to verify the assignments of the quinoid ring vibrations in the DABA–Zn complexes.

The (^{18}O)DABA compound was used to prepare the (^{18}O)DABA–Zn complex in both methylene chloride and diethyl ether and the TCI complex in $H_2{}^{16}O$ and in $H_2{}^{18}O$ buffer. The frequency changes observed in $^{16}O \rightarrow {}^{18}O$ substitution are given in Tables II and III for DABA and DABA–Zn in methylene chloride and diethyl ether, respectively, and Table IV gives the frequencies for the (^{18}O)-DABA–LADH–NADH intermediates in $H_2{}^{18}O$. If one uses a simple C–O diatomic oscillator model, a ^{12}C–^{18}O oscillator should have a frequency 97.59% that of the ^{12}C–^{16}O oscillator.

If one assigns the DABA Raman bands at 1696 cm^{-1} in diethyl ether solution and 1666 cm^{-1} in methylene chloride to an environmentally shifted carbonyl vibration, then one calculates a shift of about 40 cm^{-1} for each of these frequencies upon $^{16}O \rightarrow {}^{18}O$ substitution. The calculated frequencies for the DABA carbonyl are 1655 cm^{-1} in diethyl ether and 1623 cm^{-1} in methylene chloride. The agreement is quite remarkable for (^{18}O)DABA in diethyl ether where the observed band occurs at 1656 cm^{-1}, only 1 cm^{-1} from the calculated value of 1655 cm^{-1}. This remarkable shift of 40 cm^{-1} upon $^{16}O \rightarrow {}^{18}O$ substitution in diethyl ether indicates that in diethyl ether, the vibration of the DABA carbonyl group is not coupled to the benzene ring vibration. For DABA in methylene chloride however, the observed frequency is at 1646 cm^{-1}, a shift of only 20 cm^{-1}, indicating that it is a mixed carbonyl and ring vibration. The band at 1623 cm^{-1} in the DABA–Zn complex shifts only 5 cm^{-1} in methylene chloride and not at all in the TCI upon $^{16}O \rightarrow {}^{18}O$ substitution (see Tables II–IV). This supports our conclusion for the disappearances of the carbonyl bond upon Zn complex formation (see Discussion).

There is a band at 1402 cm^{-1} in the Zn–DABA complex in CH_2Cl_2 which goes to 1383 cm^{-1} (a 9-cm^{-1} shift) upon $^{16}O \rightarrow {}^{18}O$ substitution while in the LADH–NADH–(^{18}O)DABA TCI the shift of this band in $H_2{}^{18}O$ is from 1396 to 1390 cm^{-1} (a 6-cm^{-1} shift) (see Table IV for the ^{18}O frequencies of the TCI). However, in $H_2{}^{16}O$, the LADH–NADH–(^{18}O)DABA gives a Raman spectrum essentially identical with that of the ordinary TCI with (^{16}O)DABA since no changes greater than ±2 cm^{-1} are observed. From this, we conclude that the aldehyde oxygen in the TCI is labile with respect to $^{16}O \rightarrow {}^{18}O$ exchange.

In the zinc–DABA complex in organic solvents, the low-frequency bands which appear at 383 cm^{-1} in CH_2Cl_2 and at 394 cm^{-1} in ether do not change more than three wavenumbers upon $^{16}O \rightarrow {}^{18}O$ substitution. Thus, they must be assigned to primarily a ring vibration which is resonance enhanced upon zinc binding. The zinc–oxygen interaction could be involved if the normal mode structure is sufficiently complex. It is difficult to say exactly what this vibration could be since bond stretching vibrations are the ones which usually show the most resonance enhancement. Zinc complexes of diethylaminobenzaldehyde show an even more intense band at 390 cm^{-1} in organic solvents and the TCI. Thus, it cannot be a vibration which involves the methyl groups on the nitrogen.

It was of interest to see what type of complex is formed with LADH–NAD^+–DABOL mixtures in excess enzyme. We began with the study of the absorption spectra, at pH 9.6, of such mixtures and found an intense absorption band at 380 nm which indicated that NADH and DABA–zinc quinoid form were present. This result was unexpected since when the same experiment is done with catalytic amounts of enzyme, the conversion of DABOL–NAD^+ to DABA–NADH represents no more than a few percent of the starting material. Thus, it appears that on the enzyme surface much of the NAD^+ is reduced to NADH while the alcohol is oxidized to the zinc–aldehyde complex previously observed with DABA.

As a confirmation that the ternary complex in excess enzyme made with NAD^+–DABOL is identical with that made with NADH–DABA, the Raman spectrum of a mixture at pH 9.6, of NADH–NAD^+–DABOL in the relative concentrations 1.4×10^{-3}, 1.0×10^{-3}, and 0.7×10^{-3} M, respectively, gave a Raman spectrum identical with that previously obtained with LADH–NADH–DABA. Since the equilibrium is rather complex and we only wish to show the existence of some of the ternary complex, the laser line at 457.9 nm was used to increase the resonance enhancement of the ternary complex. This line has the advantage of increasing the Raman sensitivity to the TCI, which is the most red shifted of the possible components in the solution, but has the disadvantage that because this laser line is weaker the noise level is increased slightly. Figure 6 shows the comparison of the Raman spectrum of the tertiary complex with excess LADH formed from DABOL–NAD^+ with that obtained by using DABA–NADH. In each case, both Raman spectra are taken with

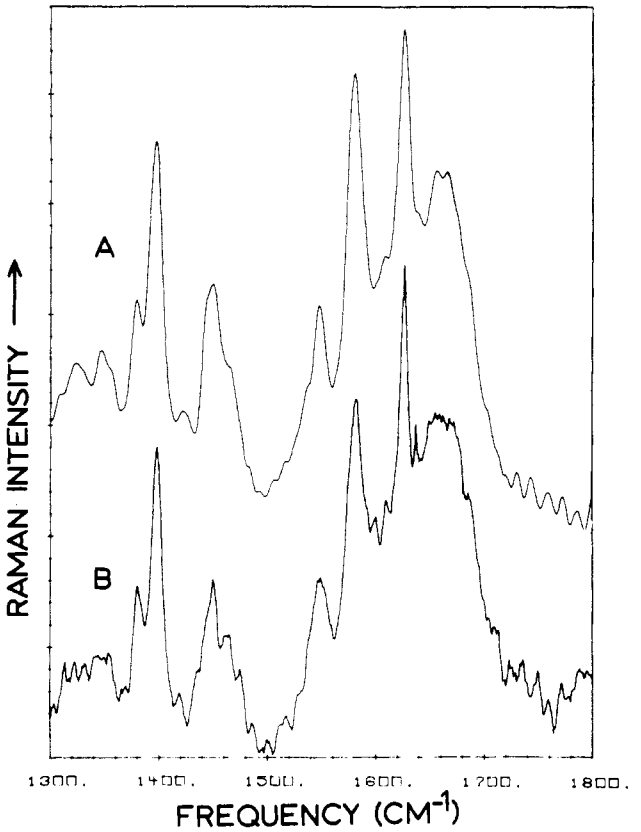

FIGURE 6: Comparison of the Raman spectrum of the ternary complex formed from the mixture LADH–NAD^+–DABOL with that obtained from the mixture LADH–$NADH^+$–DABA. In each case, the respective concentrations are 1.4×10^{-3}, 1×10^{-3}, and 0.7×10^{-3} M. For enhancement of the resonance effect, the spectra were taken with 100 mW at the sample of 457.9 nm.

457.9-nm argon laser lines. As may be seen, the two Raman spectra are identical, which demonstrates clearly that the ternary complex is the same in both cases. This means that on the enzyme surface the NAD^+ is reduced to NADH, while the alcohol is oxidized to the zinc–aldehyde complex previously observed with DABA.

Finally, in order to investigate any possible differences that might exist between the nature of the ternary intermediate that might exist in the crystalline LADH in solution, we made crystals of the LADH–NADH–DABA tertiary complex, and the Raman spectrum was taken. The Raman spectrum of the crystalline ternary intermediate was found to be identical with that in solution. Figure 7 gives the Raman spectrum of small crystals of the LADH–NADH–DABA prepared as described above. Again, the quinoid form marker bands are present.

Discussion

One of the remarkable features of the carbonyl vibration in DABA is that the frequency of the vibration is very sensitive to the dielectric constant of the solvent. The frequency goes from 1696 cm^{-1} in diethyl ether to 1667 cm^{-1} in methylene chloride to 1648 cm^{-1} in water (at concentrations much higher than that shown in Figure 1). We interpret this to be due to the increasing polarization of the carbonyl in going from R—C(H)=O to $R-C^+(H)-O^-$ in solvents of increasing dielectric content. Thus, the decrease in the frequency of the carbonyl of about 50 cm^{-1} in going from ether solution to aqueous solution is interpreted in terms of a decreasing bond order due to polarization of the C=O bond. Considering its high degree of polarizability, it is not too surprising that upon formation of an inner shell complex with zinc that the carbonyl

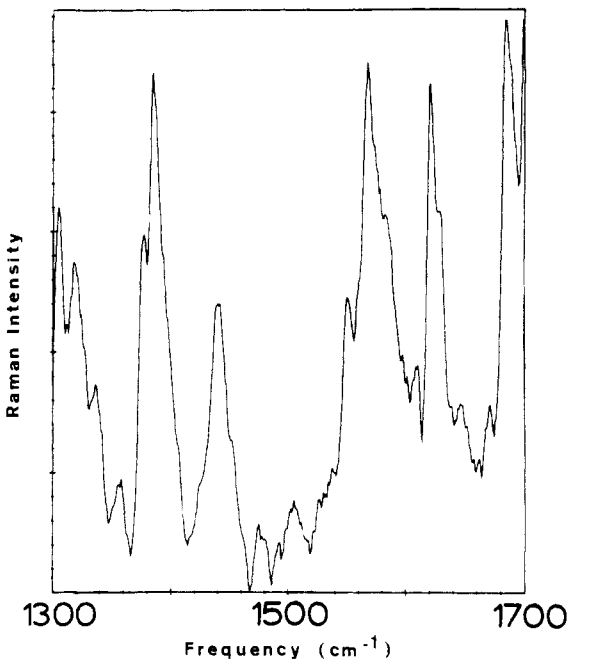

FIGURE 7: Raman spectrum of crystals of the LADH–NADH–DABA complex taken with 100 mW at 514.5 nm.

bond disappears completely as the —C(H)=O double bond is now apparently replaced by $-C^+(H)-O-Zn^+-$ bonding. It seems highly unlikely that such a major change in the DABA Raman spectrum would occur unless the DABA were forming an inner shell complex with the zinc. Thus, all of the Raman evidence supports the conclusion of a zinc–oxygen bond.

It is worthwhile to examine more carefully the possibility that the band at 1623 ± 3 cm^{-1} which appears in all of the DABA–Zn complexes in both organic solvents and the TCI in aqueous solution and which we have assigned as a quinoid marker band is not in fact due to a further decrease in the carbonyl frequency upon polarization of the carbonyl group by the zinc ion. However, an examination of the change in the frequencies of the quinoid marker bands upon $^{16}O \rightarrow {}^{18}O$ substitution in the DABA–Zn couple (see Tables II–IV) shows that the 1623-cm^{-1} band only shifts 5 cm^{-1} in the model complex in methylene chloride and does not shift at all in the (^{18}O)DABA TCI in $H_2{}^{18}O$. Other quinoid marker bands such as the bands at 1384, 1393, and 1587 cm^{-1} shift as much or more. Thus, though ^{18}O substitution leads to small shifts in the quinoid marker bands indicative of the involvement of the ^{18}O atom in some of the quinoid ring vibration, it seems clear that the 1623-cm^{-1} band is not a carbonyl vibration. Furthermore, 1623 cm^{-1} is the frequency of a resonance-enhanced Raman band always found in quinoid structures. For example, an examination of the resonance Raman spectra of five acid–base indicators of the azo dye type by Machida et al. (1974) shows virtually the same quinoid marker bands as those observed here when the dyes are in their acid or quinoid form. Particularly pronounced is a strong band which occurs at 1623 cm^{-1} which they assign to the C=C vibrations of the quinoid ring.

Although we have discussed the zinc–DABA complex as a static structure involving the formation of the Zn–O–quinoid ring structure, the tendency of the DABA oxygen to $^{18}O \rightarrow {}^{16}O$ exchange in the presence of Zn^{II} gives rise to the concept of a dynamical structure. As we have noted (see Tables III and IV), Zn–(^{18}O)DABA complex either in the enzyme pocket or in ether undergoes rapid and complete exchange to the Zn–(^{16}O)DABA complex.

This exchange does not occur in dry methylene chloride (see Table II). We did not realize the ether apparently had picked up moisture until we found evidence for $^{18}O \rightarrow {}^{16}O$ exchange in the ether solution of the Zn–(^{18}O)DABA complex. Since $ZnCl_2$ is very hydroscopic, the ether solution is very difficult to keep dry while the methylene chloride solution, being more hydrophobic, is not. However, if $H_2{}^{16}O$ is added in trace amounts to the methylene chloride solution of Zn–(^{18}O)-DABA, the ^{18}O frequency shifted the bands at 1621, 1587, 1393, and 1374 cm^{-1} [see the Zn–(^{16}O)DABA values reported earlier (Jagodzinski & Peticolas, 1981) for dry methylene chloride]. But even in very wet ether, (^{18}O)DABA does not exhibit exchange in the absence of zinc on the time scale of our experiments (several hours to a day). Thus, we may conclude when $H_2{}^{16}O$ and the Zn–(^{18}O)DABA complex are both present, $^{18}O \rightarrow {}^{16}O$ exchange occurs, but (^{18}O)DABA does not undergo this rapid exchange in the presence of $H_2{}^{16}O$ without zinc.

Since the Zn–DABA complex is formed in methylene chloride where no water is present, the zinc must form an inner shell complex with the DABA in which no water is involved. The fact that the quinoid form Raman marker bands are essentially the same for the Zn–(^{16}O or ^{18}O)DABA complex in dry methylene chloride and the TCI in $H_2{}^{16}O$ or $H_2{}^{18}O$ is again evidence that the zinc is bound directly to the oxygen of the DABA in the TCI.

Since $^{18}O \rightarrow {}^{16}O$ exchange occurs rapidly in the TCI with (^{18}O)DABA in the presence of $H_2{}^{16}O$, we conclude that the complex is a dynamic one and that for a small fraction of the time a complex involving both $H_2{}^{16}O$ and ^{18}O must be present in order to provide a reasonable mechanism for $^{18}O \rightarrow {}^{16}O$ exchange. Such transient complexes would not show up in the resonant Raman effect because their concentration is too low. However, consideration of the dynamic aspects of this ternary intermediate which are implied by the $^{18}O \rightarrow {}^{16}O$ exchange may help to resolve the differences between the NMR and the optical spectroscopic points of view.

It is tempting to assign a covalent bond between the Zn and oxygen atoms. However, studies on metal–oxygen bonds in crystalline metal hydroxides dating back over 30 years (Mathieu, 1950) show clearly that the bonding forces between metal and oxygen can be Coulombic (or ionic) and dispersive as well as covalent. For this reason, we cannot at the present time assign a definite type of bonding; however, the bond between the zinc and the oxygen is sufficiently strong to remove electrons from the carbon–oxygen double bond of the substrate.

The coordination number of the zinc in this ternary complex is still unknown. If the substrate displaces the hydrogen-bonded water molecule of the holoenzyme, then the coordination number would remain at 4. However, if the substrate binds in addition to the hydrogen-bonded ligand, this would increase the coordination number to 5. In order to see if bound water at the zinc site in any way affected the vibrational frequencies of the ternary complex, the TCI was made and the spectrum taken in D_2O. Even after deuterium–hydrogen exchange, the resonance-enhanced Raman spectrum showed no frequency shifts either at low or at high frequencies, which could be interpreted as an interaction of solvent between the metal ion and the substrate.

The fact that the TCI can be made by starting with either the reduced substrate and oxidized coenzyme or the reduced coenzyme and oxidized substrate indicates that in solutions of excess enzyme and coenzyme this ternary intermediate is a low point in the free-energy reaction coordinate between the aldehyde–NADH reactant and the alcohol–NAD^+ product. Such an observation is not without precedence in enzyme chemistry. For example, formation of stabilized enzyme–substrate intermediates for 3-phosphoglycerate kinase has been achieved by maintaining the enzyme at a concentration exceeding catalytic concentrations (Rao et al., 1978). With an enzyme to substrate ratio of approximately 1, these authors found that the equilibrium constant between product and reactant was different by a factor of 10^3 as compared to systems with the enzyme in catalytic concentration.

In our case, we may imagine a series of equilibria between at least four possible states on the enzyme surface formed among at least five reaction equilibria:

$$NAD^+ + RCH_2OH + Zn^{2+}\text{–LADH} \rightleftarrows NAD^+/RCH_2OH/Zn^{2+}\text{–LADH} \quad (1)$$

$$NAD^+/RCH_2OH/Zn^{2+}\text{–LADH} \rightleftarrows NAD^+/RCH_2O\text{–}Zn^{+}\text{–LADH} + H^+ \quad (2)$$

$$NAD^+/RCH_2O\text{–}Zn^{+}\text{–LADH} \rightleftarrows NADH/R^+CHO\text{–}Zn^{+}\text{–LADH} \quad (3)$$

$$NADH/R^+CHO\text{–}Zn^{+}\text{–LADH} \rightleftarrows NADH/RCHO/Zn^{2+}\text{–LADH} \quad (4)$$

$$NADH/RCHO/Zn^{2+}\text{–Enz} \rightleftarrows NADH + RCHO + Zn^{2+}\text{–LADH} \quad (5)$$

Equation 1 corresponds to simple absorption of the coenzyme and substrate. Equation 2 corresponds to displacements of the alcohol proton by the catalytic zinc to form the zinc alcoholate. Equation 3 corresponds to hydride transfer from the alcoholate to the NAD^+ while eq 4 corresponds to displacement of the aldehyde from the TCI and represents formation of the aldehyde–NADH mixture simply absorbed on the enzyme which dissociates (eq 5) to give the free components. In the presence of excess enzyme at pH 9.6, the equilibria produce sufficient TCI, the product in equilibrium (eq 3) as written above, so that this species is easily detected in the resonance Raman spectrum. This TCI is formed from either the NADH–DABA or the NAD^+–DABOL initial starting mixtures in excess enzyme. The TCI is the only species that is sufficiently red shifted to be resonance enhanced as the other compounds lack the quinoid-like structure. We are unable to detect the existence of the other possible components either because their concentration is too low or because their absorption bands lie too far to the ultraviolet so that the Raman intensity is too weak. However, the fact that one obtains a strong resonance in the enhanced Raman spectrum of the TCI from both DABOL–NAD^+ and DABA–NADH mixtures in the presence of excess enzyme is strong evidence that this is the major component. Thus, it appears that the TCI is a true chemical intermediate which must also exist at catalytic concentrations of the protein and is evidently poised to proceed in either the forward or the reverse direction along the reaction coordinate, depending on the equilibrium constant and on the concentrations of the products relative to those of the reactants in the bulk solution. This unexpected stability of this complex can be attributed to the strong affinity which DABA has for the divalent zinc cation.

It also seems likely that another ternary chemical intermediate, LADH–NAD^+–RCH_2–O–Zn, which involves NAD^+ and the zinc alcoholate may also be present along with the reaction pathway. We cannot say at the present time what exactly the relative concentrations of the zinc alcoholate to the zinc–aldehyde intermediates are on the protein surfaces,

but the fact that the alcohol–NAD^+ complex on the LADH surface gives essentially the same resonance–enhanced Raman spectrum as the aldehyde–NADH complex indicates that this latter complex is present in considerable excess. Unfortunately, aromatic metal alcoholates possess the same ultraviolet absorption as the aromatic alcohols, and there appears to be no way one can obtain a resonance-enhanced Raman spectrum if these materials are in the presence of protein.

The fact that the resonance-enhanced Raman spectra of the TCI crystals were identical with those of the TCI in solution further supports the conclusions of the X-ray work previously cited that a zinc–oxygen bond is involved in catalysis.

References

Angelis, C. T., Dunn, M. F., Muchmore, D. C., & Wing, R. M. (1977) *Biochemistry 16*, 2922.

Boiwe, T., & Brändén, C.-I. (1977) *Eur. J. Biochem. 77*, 173.

Bowman, W. D., & Spiro, T. G. (1980) *J. Raman Spectrosc. 9*, 369.

Brändén, C.-I., & Eklund, H. (1978) *Ciba Found. Symp. 60*, 63–80.

Brändén, C.-I., & Eklund, H. (1980) *Dehydrogenases Requiring Nicotinamide Coenzymes* (Jeffrey, J., Ed.) pp 441–484, Birkhäuser Verlag, Basel and Boston.

Carey, P. R. (1978) *Q. Rev. Biophys. 3*, 309–370.

Drysdale, B.-E., & Hollis, D. P. (1980) *Arch. Biochem. Biophys. 205*, 267.

Dunn, M. F., & Hutchison, J. S. (1973) *Biochemistry 12*, 4882.

Dunn, M. F., Biellmann, J.-F., & Branlant, G. (1975) *Biochemistry 14*, 3176.

Dunn, M. F., Bernhard, S. A., Anderson, D., Copeland, A., Morris, R. G., & Roque, J.-P. (1979) *Biochemistry 18*, 2346.

Dworschack, R. T., & Plapp, B. V. (1977) *Biochemistry 16*, 2716.

Eklund, H., Samama, J.-P., Wallén, L., Brändén, C.-I., Åkeson, Å., & Jones, T. A. (1981) *J. Mol. Biol. 146*, 561–587.

Fersht, A. (1977) *Enzyme Structure and Mechanism*, p 293, W. H. Freeman, San Francisco.

Forster, M., Girling, R. B., & Hester, R. E. (1980) *Proceedings of the International Conference of Raman Spectroscopy* (Murphy, W. F., Ed.) p 316, North-Holland Publishing Co., New York.

Gaber, B. P., Yager, P., & Peticolas, W. L. (1978) *Biophys. J. 21*, 161.

Honig, B. (1978) *Annu. Rev. Phys. Chem. 29*, 31–57.

Jagodzinski, P. W., & Peticolas, W. L. (1981) *J. Am. Chem. Soc. 103*, 234.

Kim, B. K., Kagayawa, A., Saito, Y., Machida, K., & Uho, T. (1975) *Bull. Chem. Soc. Jpn. 48*, 1394–1396.

Klotz, I. M., Burkhard, R. K., & Urquhart, J. M. (1952) *J. Am. Chem. Soc. 74*, 202.

Koerber, S. C., Schack, P., Aug, A. M.-J., & Dunn, M. F. (1980) *Biochemistry 19*, 731.

Kvassman, J., & Pettersson, G. (1978) *Eur. J. Biochem. 87*, 417.

Kvassman, J., & Pettersson, G. (1980a) *Eur. J. Biochem. 103*, 557.

Kvassman, J., & Pettersson, G. (1980b) *Eur. J. Biochem. 103*, 565.

Loader, J. (1970) *Basic Laser Raman Spectroscopy*, p 27, Heyden & Son Ltd., London.

Lord, R. C. (1977) *Appl. Spectrosc. 31*, 187–194.

Lord, R. C., & Yu, N. T. (1970) *J. Mol. Biol. 50*, 509.

Machida, K., Kim, B. K., Saito, Y., Igarashi, K., & Uho, T. (1974) *Bull. Chem. Soc. Jpn. 47*, 78–83.

Mathieu, J.-P. (1950) *C. R. Hebd. Seances Acad. Sci. 231*, 896–897.

McFarland, J. T., Watters, K. L., & Petersen, R. L. (1975) *Biochemistry 14*, 624.

Morris, R. G., Saliman, G., & Dunn, M. F. (1980) *Biochemistry 19*, 725.

Nakamoto, K. (1978) *Infrared and Raman Spectra of Inorganic and Coordination Compounds*, Wiley, New York.

Peticolas, W. L., & Klotz, L. M. (1956) *J. Am. Chem. Soc. 78*, 5257.

Plapp, B. V., Eklund, H., & Brändén, C.-I. (1978) *J. Mol. Biol. 122*, 23–32.

Rao, B. D. N., Cohn, M., & Scopes, R. K. (1978) *J. Biol. Chem. 253*, 8056–8060.

Rodgers, E. G., & Peticolas, W. L. (1980) *J. Raman Spectrosc. 9*, 372.

Savitski, A., & Golay, J. E. (1964) *Anal. Chem. 36*, 1627.

Simons, L., Bergström, G., Blomfelt, G., Forss, S., Stenbäck, H., & Wansen, G. (1972) *Commentat. Phys.-Math. 42*, 125.

Sloan, D. L., Young, J. M., & Mildvan, A. S. (1975) *Biochemistry 14*, 1998.

Spiro, T. G., & Gaber, B. P. (1977) *Annu. Rev. Biochem. 46*, 533.

Theorell, H., & Chance, B. (1951) *Acta Chem. Scand. 5*, 1127.

Theorell, H., & McKinley McKee, J. S. (1961a) *Acta Chem. Scand. 15*, 1811.

Theorell, H., & McKinley McKee, J. S. (1961b) *Acta Chem. Scand. 15*, 1834.